# Autosomal Dominant Diabetes Arising From a Wolfram Syndrome 1 Mutation

**Lori L. Bonnycastle,[1] Peter S. Chines,[1] Takashi Hara,[2] Jeroen R. Huyghe,[3] Amy J. Swift,[1] Pirkko Heikinheimo,[4] Jana Mahadevan,[2] Sirkku Peltonen,[5] Hanna Huopio,[6] Pirjo Nuutila,[7,8] Narisu Narisu,[1] Rachel L. Goldfeder,[1] Michael L. Stitzel,[1] Simin Lu,[2] Michael Boehnke,[3] Fumihiko Urano,[2] Francis S. Collins,[1] and Markku Laakso[9]**

We used an unbiased genome-wide approach to identify exonic variants segregating with diabetes in a multigenerational Finnish family. At least eight members of this family presented with diabetes with age of diagnosis ranging from 18 to 51 years and a pattern suggesting autosomal dominant inheritance. We sequenced the exomes of four affected members of this family and performed follow-up genotyping of additional affected and unaffected family members. We uncovered a novel nonsynonymous variant (p.Trp314Arg) in the Wolfram syndrome 1 (*WFS1*) gene that segregates completely with the diabetic phenotype. Multipoint parametric linkage analysis with 13 members of this family identified a single linkage signal with maximum logarithm of odds score 3.01 at 4p16.2-p16.1, corresponding to a region harboring the *WFS1* locus. Functional studies demonstrate a role for this variant in endoplasmic reticulum stress, which is consistent with the β-cell failure phenotype seen in mutation carriers. This represents the first compelling report of a mutation in *WFS1* associated with dominantly inherited nonsyndromic adult-onset diabetes.
***Diabetes* 62:3943–3950, 2013**

Considerable advances have been made in our understanding of the genetics of monogenic diabetes, which accounts for 1–3% of diabetes cases (1–3). The identification of causative genetic variants responsible for monogenic diabetes has revealed critical elements of the pathways involved in insulin and glucose metabolism, and in some instances has led to important therapeutic interventions (4). But the list of ~20 known causative loci for monogenic diabetes is far from complete, as DNA sequencing of known genes has failed to identify mutations in some families (1). The overlap of genes identified in genome-wide association studies and/or candidate gene studies of the more common type 2 diabetes with those of the known monogenic diabetes genes suggests that common genetic pathways may be involved (4). Thus, identifying the as-yet-undefined genes involved in monogenic diabetes would also offer new insights into the genetics of type 2 diabetes.

We set out to identify the genetic cause of diabetes in a four-generation family with an apparent autosomal dominant form of adult-onset diabetes (Fig. 1). Previous sequencing of the exons of known maturity-onset diabetes of the young (MODY) genes in a subset of the affected members of this family failed to identify candidate variants segregating with diabetes. Thus, we sequenced the exomes of four affected members of this family, with follow-up screening of additional affected and unaffected family members, and uncovered a novel nonsynonymous variant in the Wolfram syndrome 1 (*WFS1*) gene as the likely causative mutation for diabetes in this family.

## RESEARCH DESIGN AND METHODS

**Study participants.** Informed consent was obtained from study participants, and the respective institutional review boards for the participating institutions each approved this study. The first participants from this family entered the study through the genetic diagnostic services at the University of Eastern Finland. Blood samples were taken for DNA extraction. Four of the family members underwent an oral glucose tolerance test (a 75-g glucose load). Plasma glucose levels were determined with the glucose oxidase method, plasma insulin and C-peptide levels by time-resolved immunofluorometric assay, and serum glutamic acid decarboxylase (GAD) autoantibodies by ELISA.

**Exome sequencing and sequence analysis.** Multiplexed, paired-end DNA libraries were prepared for targeted exome capture and sequencing as previously described (5), with minor modifications. In brief, 1.5 μg of genomic DNA fragmented to an average of 300 bp was end repaired, ligated to adapters containing a six-base index sequence, and PCR amplified. Targeted capture of exome sequences from libraries was performed with the Roche NimbleGen SeqCap EZ Exome Library v2.0 and sequenced on the Illumina HiSeq2000 as described by the manufacturer's protocols for paired 101-bp reads.

Reads passing the Illumina "chastity filter" were aligned to the UCSC hg19 genome assembly (pseudoautosomal region on Y chromosome masked, alternative haplotypes removed) using Novoalign v2.07.18 (http://www.novocraft.com), and duplicate read pairs were removed. Genotypes for single nucleotide polymorphisms (SNPs) and short indels were called using a Bayesian approach implemented in most probable genotype (5) and filtered using a score threshold of 10 and a score/depth ratio threshold of 0.5.

Variants were annotated using Annovar (6) and coding transcripts from GencodeV7 (7). Allele frequencies for each variant were estimated based on phase 1 genotypes from the 1000 Genomes project (8), the European Americans among the 6,500-exome release of the National Heart, Lung, and Blood Institute (NHLBI) GO Exome Sequencing Project (http://evs.gs.washington.edu/EVS/), and the Finnish whole-exome data from the T2D-GENES (Type 2 Diabetes Genetic Exploration by Next-generation sequencing in multi-Ethnic Samples) consortium.

**Genotyping with HumanOmni2.5-8 BeadChip.** Samples were genotyped with the Illumina HumanOmni2.5-8 BeadChip according to the manufacturer's protocols; genotypes were called using BeadStudio with standard cluster definitions. To obtain the most accurate SNP positions and allele orientations, Illumina probe sequences were mapped to the hg19 genome assembly using

From the [1]National Human Genome Research Institute, Bethesda, Maryland; the [2]Department of Medicine and Department of Pathology and Immunology, Washington University School of Medicine, St. Louis, Missouri; the [3]Department of Biostatistics and Center for Statistical Genetics, School of Public Health, University of Michigan, Ann Arbor, Michigan; the [4]Department of Biochemistry and Food Chemistry, University of Turku, Turku, Finland; the [5]Department of Dermatology, University of Turku, Turku, Finland; the [6]Department of Paediatrics, Kuopio University Hospital, Kuopio, Finland; the [7]Department of Medicine and Turku PET Centre, University of Turku, Turku, Finland; the [8]Department of Medicine and Turku PET Centre, Turku University Hospital, Turku, Finland; and the [9]Department of Medicine, University of Eastern Finland and Kuopio University Hospital, Kuopio, Finland.

Corresponding author: Francis S. Collins, collinsf@mail.nih.gov.
Received 10 April 2013 and accepted 26 July 2013.
DOI: 10.2337/db13-0571
© 2013 by the American Diabetes Association. Readers may use this article as long as the work is properly cited, the use is educational and not for profit, and the work is not altered. See http://creativecommons.org/licenses/by-nc-nd/3.0/ for details.

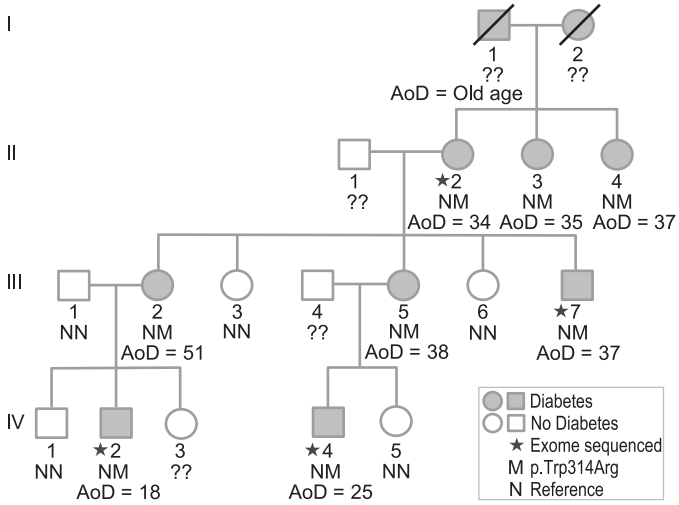


**FIG. 1. Pedigree of four-generation (I–IV) family with autosomal dominant diabetes and WFS1 p.Trp314Arg carrier status. Gray squares and circles, patients with diabetes; white squares and circles, normal glucose tolerant. AoD, age of diagnosis of diabetes; M, p.Trp314Arg variant; N, reference allele; ?, unknown; *exome sequenced.**

Burrows-Wheeler Aligner v0.5.8c (9), which lead to the exclusion of 32,622 SNPs due to various alignment problems: no alignment, multiple alignments, or presence of known variants near 3′ end of probes.

**Quality-control analysis.** Comparison of genotypes called from the exome data with those also called on the HumanOmni2.5-8 BeadChip for each individual showed a mean concordance of 99.60% overall ($n$ = 123,376–126,328), 99.83% in coding regions ($n$ = 63,929–64,093) and 99.48% at heterozygous sites on the BeadChip in coding regions ($n$ = 8,043–8,261).

**Variant validation and screening for variants in additional family members.** Sanger sequencing (ACGT, Wheeling, IL) was used as an alternate platform to validate candidate variants in the four exome-sequenced individuals. Follow-up genotyping was performed to screen for validated variants in additional family members. The *WFS1* variant was genotyped with the Applied Biosystems TaqMan Allelic Discrimination Assay, and the *TNN* variant was genotyped with Sanger sequencing.

**Sanger sequencing of the *WFS1* promoter, 5′ untranslated region, and nearby regulatory regions.** *WFS1* regions potentially harboring the promoter (upstream of the 5′ untranslated region [UTR]) or regulatory elements such as enhancers/insulators (5′ UTR/exon 1 and intron 1) were Sanger sequenced (ACGT). The coordinates of the region targeted for sequencing (hg19; chr4: 6,270,603–6,272,808) were defined by chromatin marks (H3K4me3 and H3K27ac) predictive of an "active promoter" state at *WFS1* across 10 cell lines consisting of nine ENCODE cell types (10) and islets (M.L.S., unpublished data). Five amplicons were sequenced to cover this 2.20-kb region, which includes 0.973 kb upstream of the 5′ UTR, the 5′ UTR (exon 1, 0.165 kb), and 1.067 kb into intron 1.

**Linkage analysis.** Genotype data from the Illumina Omni2.5-8 BeadChip for 13 family members were available for linkage analysis. Sample-level quality control was performed with PLINK (11) and included checks for sample contamination and verification of pedigree structure and sex.

SNPs with missing genotypes or Mendelian inconsistencies identified using Pedstats (12) were excluded. A subset of SNPs informative for linkage analysis was selected by first retaining SNPs with at least seven copies of the minor allele in the 13 genotyped subjects and then dividing chromosomes into 100-kb segments and selecting the first SNP located at least 75 kb away from the previous adjacent SNP. This resulted in a map of 25,303 autosomal SNPs with a median intermarker distance of 99 kb. Remaining possible genotyping errors were detected by identifying unlikely double recombinants using Merlin (13), and these SNPs were designated as missing for subsequent analysis.

Multipoint parametric linkage analysis was conducted using Merlin, assuming autosomal dominant inheritance. To assess robustness of linkage evidence to model parameters, analyses were repeated for a range of penetrance parameters. Allele frequencies were estimated by counting across all individuals, and multipoint logarithm of odds (LOD) scores were calculated along a 0.1-cM grid. The genetic map was approximated from the physical map by assuming 1 cM∼1 Mb. All positions reported are based on human genome build hg19 coordinates.

**Luciferase assay.** For reporter assays, 293T cells were cotransfected with the endoplasmic reticulum (ER) stress response element (ERSE) (rat promoter GRP78)–luciferase construct (14) and various constructs as indicated. Prior to lysis at 24 h after transfection, cells were treated with or without 10 nmol/L of thapsigargin (TG) for 6 h. Firefly luciferase activity was measured using the Dual-Luciferase Reporter Assay System (Promega, Madison, WI) and normalized to Renilla luciferase values of the cotransfected pRL-TK vector (Promega) to control for differences in transfection efficiency.

**Quantitative PCR assay for expression of *WFS1*.** Total RNA was isolated from the cells using the RNeasy Mini Kit (Qiagen) and reverse transcribed using 1 μg of total RNA from cells with Oligo-dT primer. For the thermal cycle reaction, the Vii A7 (Applied Biosystems) was used at 95°C for 10 min and then 40 cycles at 95°C for 10 s and 55°C for 30 s.

The relative amount for each transcript was calculated by a standard curve of cycle thresholds for serial dilutions of cDNA samples and normalized to the amount of β-actin. PCR was performed in triplicate for each sample, after which all experiments were repeated twice. The following sets of primers and Power SYBR Green PCR Master Mix (Applied Biosystems) were used for real-time PCR: human actin, ACCATGGATGATGATATCGCC and GCCTTGCACATGCCGG; human WFS1, GAGCCCTGAGGACCTGCC (exon 7) and TCTCCATGATGGCGTGCA (exon 8).

**Immunoblotting (Western blots).** Fibroblast cell lysates (30 μg protein equivalent) were electrophoresed at 200 V for 1 h using NuPAGE 4–12% Bis-Tris Gel (Life Technologies) and transferred to polyvinylidene fluoride membrane (iBlot; Invitrogen). The membrane was blocked for 1 h at room temperature with 5% milk in TBS-Tween, probed overnight at 4°C with primary anti-WFS1 (rabbit, 1:1,000; Cell Signaling) or antitubulin (mouse, 1:2,000; Sigma-Aldrich) antibodies, followed by 1 h incubation at room temperature with secondary horseradish peroxidase–conjugated antibody (donkey anti-rabbit, 1:10,000 [Amersham-GE Healthcare] or goat anti-mouse, 1:5,000 [Santa Cruz Biotechnology]). ECL Western blotting and analysis reagents (GE Healthcare) were used for chemiluminescent detection.

**Immunostaining.** Human skin fibroblasts were fixed in 2% paraformaldehyde for 30 min at room temperature and then permeabilized with 0.1% Triton X-100 for 2 min. The fixed cells were washed with PBS, blocked with 10% BSA for 30 min, and incubated in primary antibody overnight at 4°C. The cells were washed three times in PBS/Tween 0.1% and incubated with secondary antibody for 1 h at room temperature. Images were obtained with an FSA 100 microscope (Olympus). Anti-WFS1 antibody and anti–protein disulfide isomerase (anti-PDI) antibody were obtained from Proteintech Group (Chicago, IL) and Stressgen (Victoria, BC, Canada), respectively.

## RESULTS

**Family participants and clinical phenotypes.** Six of the eight affected family members (generations II–IV) were diagnosed with diabetes at 34–51 years of age and two (IV-2 and IV-4) at 18 and 25 years of age, respectively (Fig. 1). There is no history of ketoacidosis in any of the family members with diabetes, and seven of them are currently treated with insulin. BMI values for the eight diabetic family members ranged from 18.1 to 26.8 kg/m$^2$, with six having values <25 kg/m$^2$. Detailed clinical examination of the diabetic family members did not reveal any of the other clinical features of the Wolfram syndrome (WS) (hearing impairment in audiograms, optic atrophy or vision impairment in annual ophthalmoscopy examinations, or diabetes insipidus).

We performed an oral glucose tolerance test with measured insulin and C-peptide levels for four members of a nuclear family within this multigenerational family who were available for further characterization (Table 1). The diabetic mother and son (III-2 and IV-2) of this family had blunted insulin and C-peptide responses when challenged with a glucose load of 75 g. Residual insulin and C-peptide levels, the lack of ketoacidosis, and the absence of GAD autoantibodies exclude a diagnosis of either type 1 diabetes or latent autoimmune diabetes of adults.

**Exome sequencing of four family members.** To determine the molecular basis of diabetes in this family, we sequenced the exomes of four of the eight diabetic individuals (II-2, III-7, IV-2, and IV-4) representing three generations.

TABLE 1
Clinical and laboratory characteristics of selected family members

| Characteristics | III-2 | III-1 | IV-2 | IV-1 |
|---|---|---|---|---|
| Glucose tolerance status | Diabetes | No diabetes | Diabetes | No diabetes |
| BMI (kg/m$^2$) | 23.0 | 24.5 | 21.6 | 21.5 |
| Age of onset of diabetes (years) | 51 | — | 18 | — |
| History of ketoacidosis | No | — | No | — |
| GAD autoantibodies | No | — | No | — |
| WS* | No | — | No | — |
| Fasting glucose (mmol/L) | 7.0 | 6.2 | 14.8 | 6.0 |
| 30-min glucose (mmol/L) | 9.9 | 8.8 | 19.2 | 9.1 |
| 60-min glucose (mmol/L) | 10.4 | 6.6 | 22.2 | 7.6 |
| 120-min glucose (mmol/L) | 12.6 | 3.6 | 20.4 | 5.0 |
| Fasting insulin (mU/L) | 6.0 | 8.0 | 4.0 | 12.0 |
| 30-min insulin (mU/L) | 19.0 | 62.0 | 12.0 | 61.0 |
| 60-min insulin (mU/L) | 18.0 | 135.0 | 14.0 | 52.0 |
| 120-min insulin (mU/L) | 18.0 | 13.0 | 6.0 | 12.0 |
| Fasting C-peptide (nmol/L) | 0.64 | 0.98 | 0.50 | 0.76 |
| 30-min C-peptide (nmol/L) | 1.30 | 3.10 | 0.91 | 2.40 |
| 60-min C-peptide (nmol/L) | 1.50 | 5.40 | 1.20 | 2.80 |
| 120-min C-peptide (nmol/L) | 1.80 | 2.10 | 0.89 | 1.60 |

*No visual impairment or optic atrophy, no hearing impairment, and no diabetes insipidus.

An average of 38.8 million reads were obtained for each individual, providing coverage ≥14-fold for 90% and ≥28-fold for 80% of the protein-coding base pairs in GencodeV7 exons. A minimum of 90.5% of these bases were confidently called for each individual. In the four sequenced individuals, 153,515 variants (SNPs and small indels) were identified, with an average of 86,989 variants per person. We applied several filters to reduce and prioritize the number of variants for follow-up assessment (Table 2).

Three heterozygous missense variants in three genes fulfilled all criteria; the genes were *JMY* (junction mediating and regulatory protein, p53 cofactor), *TNN* (tenascin N), and *WFS1*. We used Sanger sequencing to validate these three variants and confirmed the presence of variants in *TNN* and *WFS1* (but not in *JMY*) in all four of the exome-sequenced patients with diabetes. We then screened additional family members (available to our study), who had not been exome sequenced, for the two validated variants. Based on the screening of additional family members, we excluded the *TNN* variant as causative, as it did not segregate with diabetes status. The remaining *WFS1* variant (c.940T>C; p.Trp314Arg) segregated completely with affection status for the 13 affected and unaffected individuals tested (Fig. 1). To our knowledge, this variant is novel and unique to this family as it has not been observed in 1000 Genomes, NHLBI exomes, or 962 Finnish samples in the T2D-GENES consortium.

TABLE 2
Variant prioritization strategy

| Filter | *n* variants |
|---|---|
| Pass primary quality-control filters | 153,515 |
| Potentially deleterious: nonsense, frameshift, missense, splice | 16,146 |
| Present in 4/4 affected family members* | 6,337 |
| Novel or rare† (allele frequency <0.02%‡) | 715 |
| Present ≤1 time in nondiabetic exomes ($n$ = 43) sequenced in laboratory | 37 |
| Low evidence for being an artifact§ | 8 |
| Low frequency in dbSNP 135 | 3 |

*Includes variants with no genotype calls in a subset of the four samples. †Based on the prevalence of MODY and a dominant genetic model. ‡Data sources: 1000 Genomes ($n$ = 1,092 samples), NHLBI exomes ($n$ = 6,500 samples), and T2D-GENES consortium Finnish exomes ($n$ = 962). §Not in DNA regions that are difficult to sequence or challenging to align to the reference genome such as segmental duplications or variants with genotype calls in <50% of exome samples sequenced in our laboratory with the same capture and sequencing technology.

**Sanger sequencing of promoter and potential regulatory regions in 5′ UTR/exon 1 and intron 1.** To rule out the contribution of variants in potentially important regulatory sites not captured by exome sequencing, we performed Sanger sequencing on all 13 members of the family, targeting an ~2.20-kb region encompassing 0.973 kb upstream of the 5′ UTR, the 5′ UTR (exon 1, 0.165 kb), and 1.067 kb into intron 1. Enrichment of histone H3 lysine 4 trimethyl (H3K4me3) and H3 lysine 27 acetylation (H3K72ac) modifications that mark active promoters and enhancers in nine ENCODE cell types and islets strongly suggests that this targeted *WFS1* region contains the promoter and potential enhancers. We obtained good quality sequence for 100% of this region and did not identify any variants segregating with diabetes status.

**Linkage analysis with 13 family members across three generations.** Taking advantage of the availability of several DNA samples from this family and to provide additional support for *WFS1* as the responsible locus, we performed parametric multipoint linkage analysis with genotype data from the Illumina HumanOmni2.5-8 chip for 13 members of this family. Assuming complete penetrance and no phenocopies under a dominant inheritance model, we observed evidence for linkage of diabetes to a single region, 4p16.2-p16.1 (maximum LOD score 3.01) (Fig. 2). Repeating this analysis with a range of penetrance parameters and nonzero phenocopy rates did not qualitatively alter these results. The ~1.6-Mb region (LOD >1.9) of this linkage peak harbors 16 genes, one of which is *WFS1*.

***WFS1* variant and ER stress.** *WFS1* mRNA is found in several cell types and is highly expressed in the pancreatic

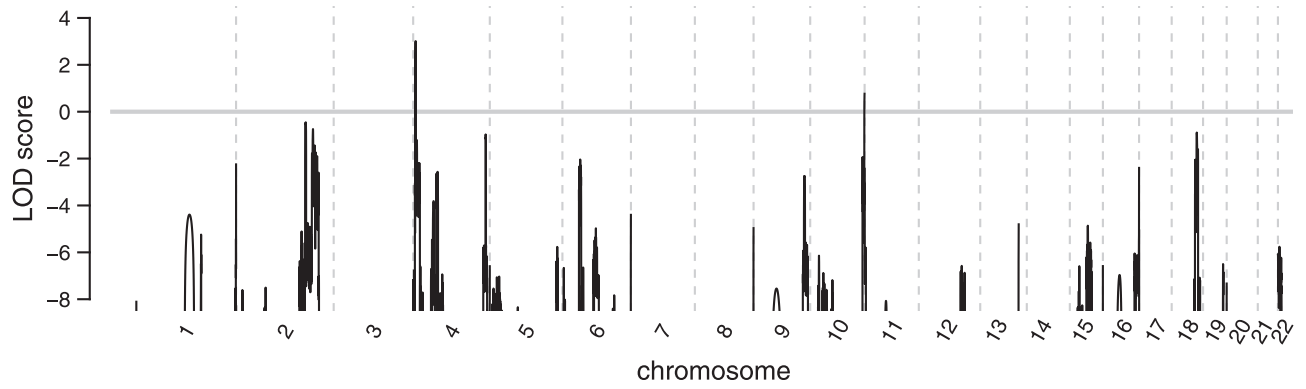


**FIG. 2. Parametric multipoint LOD scores based on pruned set of Illumina Omni2.5 SNP chip genotypes for 13 family members (Fig. 1: II-2, II-3, II-4, III-1, III-2, III-3, III-5, III-6, III-7, IV-1, IV-2, IV-4, and IV-5). A maximum LOD score of 3.01 was identified on chromosome 4p16.2-p16.1. LOD, logarithm of odds.**

β-cell (15). WFS1 participates in many important cellular processes, including insulin production, processing, and secretion; production of cyclic AMP; and regulation of ER calcium levels (as reviewed in 16,17). WFS1 also plays a role in the suppression of ER stress–mediated cell death by preventing hyperactivation of the ER stress response, raising the possibility that the p.Trp314Arg variant may cause the dysregulation of the ER stress response. To test this hypothesis, we investigated the effect of both this p.Trp314Arg variant and another rare variant (p.His313Tyr) in an adjacent codon, which was identified as de novo mutations in two unrelated Danish individuals with WS (18). With no other mutations identified in *WFS1* in these two individuals, it is reasonable to assume that p.His313Tyr is capable of causing WS in the heterozygous state. We cotransfected HEK293T cells with a luciferase reporter construct containing an ERSE and an expression vector with either *1*) control (pcDNA), *2*) wild-type *WFS1*, *3*) mutant c.937C>T *WFS1* (p.His313Tyr), or *4*) mutant c.940T>C *WFS1* (p.Trp314Arg). The ERSE reporter reflects activation levels of the ER stress response. In the absence of the ER stress inducer TG, the p.His313Tyr mutant strongly activated the ERSE reporter. After inducing ER stress with TG, both mutants p.His313Tyr and p.Trp314Arg exhibited significantly higher ERSE activity than wild-type WFS1, with the p.Trp314Arg having a milder effect (Fig. 4). This suggests that the WS-causing mutant p.His313Tyr increases ER stress, whereas the less severely affected p.Trp314Arg mutant may be pathogenic due to a defect in its ability to suppress the ER stress response after the pathway is activated.

**Functional consequences of the *WFS1* (c.940T>C; p.Trp314Arg) variant.** To further investigate the effect of the c.940T>C variant on *WFS1* transcripts and protein product, we assessed fibroblast cell lines generated from a family quartet of c.940T>C carriers and noncarriers (III-1, III-2, IV-1, and IV-2) for differences in *1*) *WFS1* transcript levels, *2*) WFS1 protein abundance, *3*) cellular localization of the WFS1 protein, and *4*) cAMP levels, which are regulated by interactions between WFS1 and adenyl cyclase 8 (19). *WFS1* mRNA expression levels were comparable in variant and nonvariant carriers (Fig. 5*A*).

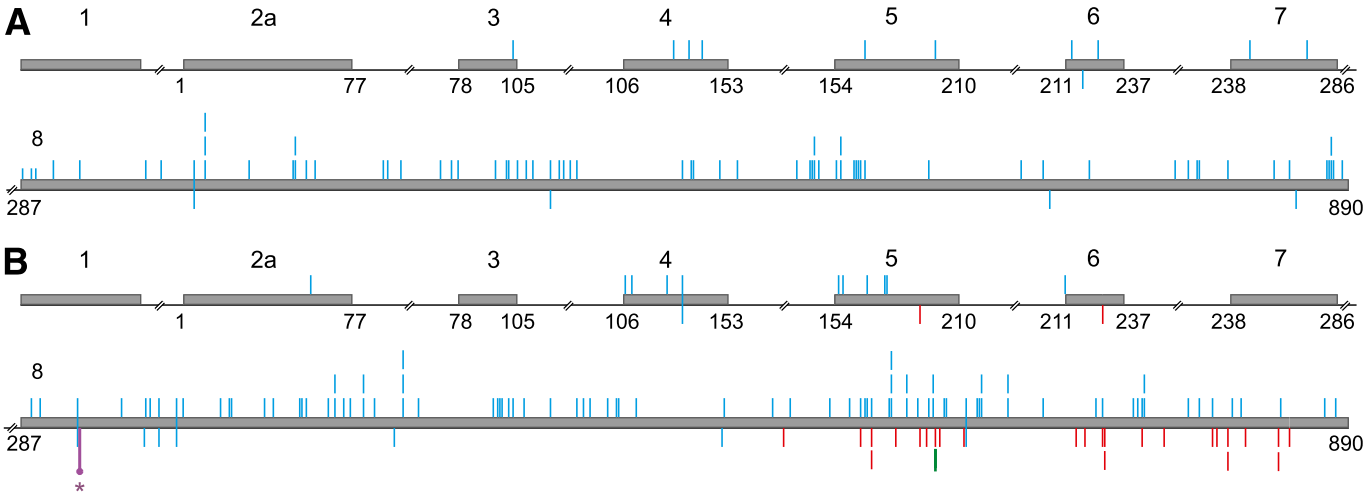


**FIG. 3. Variants in *WFS1* identified in individuals with WS, MODY, or SNHI. Variants as listed in the EURO-WABB open variation database (https://lovd.euro-wabb.org/home.php?select_db=WFS1). *A*: Nonsense or frameshift variants. *B*: Missense variants. Gray boxes are exons; tick marks extending up from exons represent variants identified in a homozygous or compound heterozygous state, and tick marks extending below exons represent variants identified as a single heterozygous variant, although some of the cases of WS may be those in which the second allele has not yet been identified. Tick marks: blue, variants in WS individuals; red, variants in SNHI individuals; green, variant p.Arg703Cys identified in MODY individual; purple with asterisks, p.Trp314Arg identified in current study showing autosomal dominant inheritance of diabetes.**

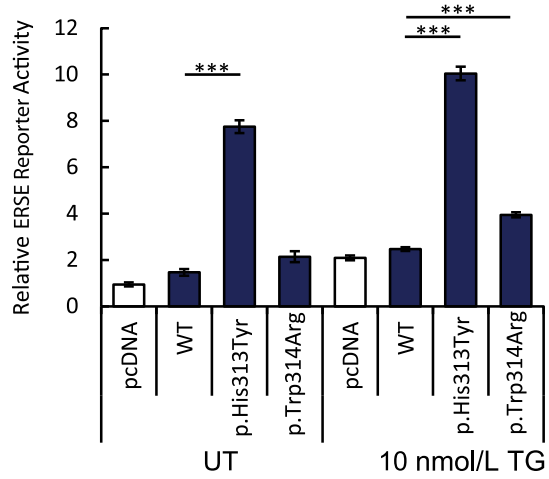


**FIG. 4. Luciferase reporter assays in HEK293T cells transfected with the ERSE reporter together with control (pcDNA), wild-type *WFS1* (WT), mutant c.937C>T *WFS1* (p.His313Tyr), or mutant c.940T>C *WFS1* (p.Trp314Arg) expression plasmid. Cells were untreated (UT) or treated with TG (10 nmol/L) for 6 h. Relative intensity of luciferase (Promega Dual-Luciferase Reporter Assay System) was then measured ($n = 3$; values are mean ± SD). Transfections were normalized with the pRL-TK vector (Promega) as an internal control. Welch *t* test on log-transformed data was used for determining the significance between two treatments. ***$P < 0.05$.**

Similarly, WFS1 protein was present in all fibroblast lysates, and protein levels did not significantly correlate with variant status (Fig. 5*B*). The variant also did not dramatically alter the subcellular localization of the WFS1 protein; both wild type and p.Trp314Arg exhibited a diffuse reticular pattern colocalizing with the ER marker PDI (Fig. 6). Lastly, cAMP levels did not correlate with carrier status of the c.940T>C; p.Trp314Arg variant (data not shown). Of note, fibroblasts generated from several WS patients carrying known causative *WFS1* variants also exhibited no differences in cAMP levels when compared with those from nonmutant *WFS1* individuals (F.U., unpublished data). Thus, the absence of an effect on *WFS1* mRNA, protein, and cAMP levels in fibroblasts suggests a resiliency of this cell type to defective or absent WFS1 and may reflect cell type–specific activities of this protein.

## DISCUSSION

We sequenced the exomes of four members of a family with dominantly inherited adult-onset diabetes and identified a single novel variant in *WFS1* correlating with disease status. Our biological interest in *WFS1* was high, as coding variants in this gene have been associated with type 1 diabetes in candidate gene studies (20,21) and common noncoding variants nearby this gene have been associated with increased risk for type 2 diabetes in genome-wide association studies (22,23). Furthermore, coding mutations in *WFS1* give rise to two major clinical phenotypes: WS (or DIDMOAD) and sensorineural hearing impairment (SNHI). WS is a rare progressive neurodegenerative disorder usually characterized by diabetes insipidus, early-onset diabetes, optic atrophy, and deafness (hence the acronym DIDMOAD), with diabetes and optic atrophy being the most consistent features (17,24). WS is an autosomal recessive disorder, with nearly all cases harboring mutations in both alleles of *WFS1* (as reviewed in 17,25) (Fig. 3*A* and *B*). In contrast, SNHI is generally inherited as an autosomal dominant condition attributable to heterozygous missense variants in this same gene (26–29).

The *WFS1* gene encodes a multispan transmembrane protein localized to the ER. Partial or complete loss of function of WFS1 protein gives rise to WS, whereas missense changes in the COOH-terminal domain typically cause SNHI (Fig. 3). The c.940T>C; p.Trp314Arg (exon 8) missense mutation identified in this report is located in the first transmembrane domain and is highly conserved (genomic evolutionary rate profiling score of 4.25) and predicted to be deleterious by several algorithms (CDPred, PolyPhen, Condel, and SIFT). Other than diabetes, the p.Trp314Arg carriers in this family had none of the other common signatures of WS, such as optic atrophy, diabetes

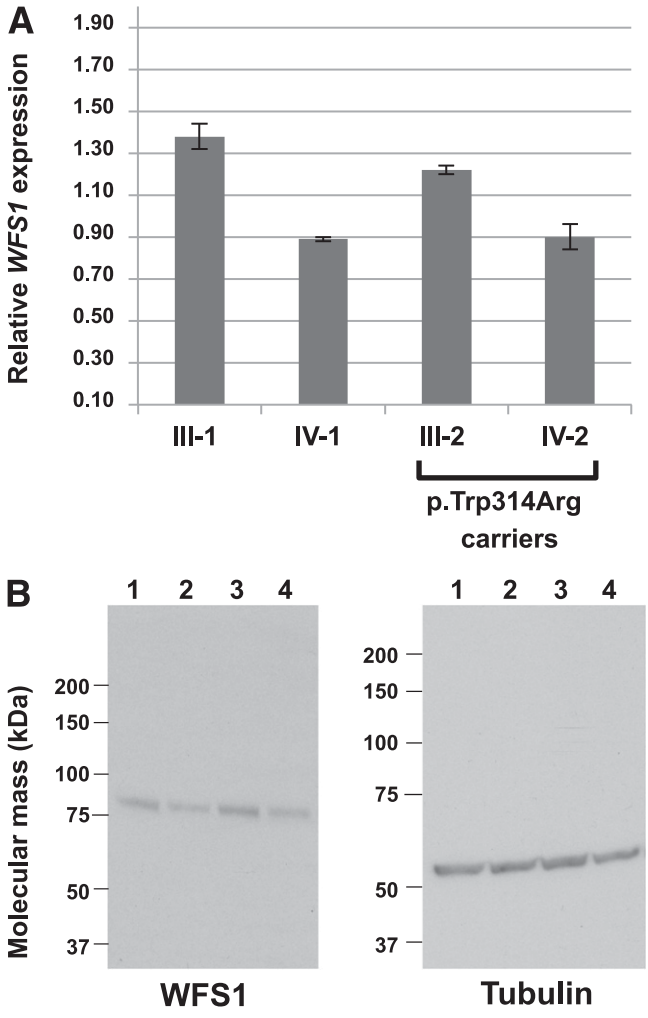


| Lane | Sample | *Relative Units |
|---|---|---|
| 1 | IV-1 | 0.67 |
| 2 | III-1 | 0.45 |
| 3 | III-2 (p.Trp314Arg) | 0.85 |
| 4 | IV-2 (p.Trp314Arg) | 0.68 |

**FIG. 5. Expression of *WFS1* in fibroblasts from c.940T>C (p.Trp314Arg) carriers and noncarriers. *A*: Expression of *WFS1* mRNA in skin fibroblasts. *B*: Western blot analysis of WFS1 protein abundance with tubulin as loading control. *Relative densitometry measurements (WFS1/tubulin) made with ImageJ64 (http://imagej.nih.gov/ij).**

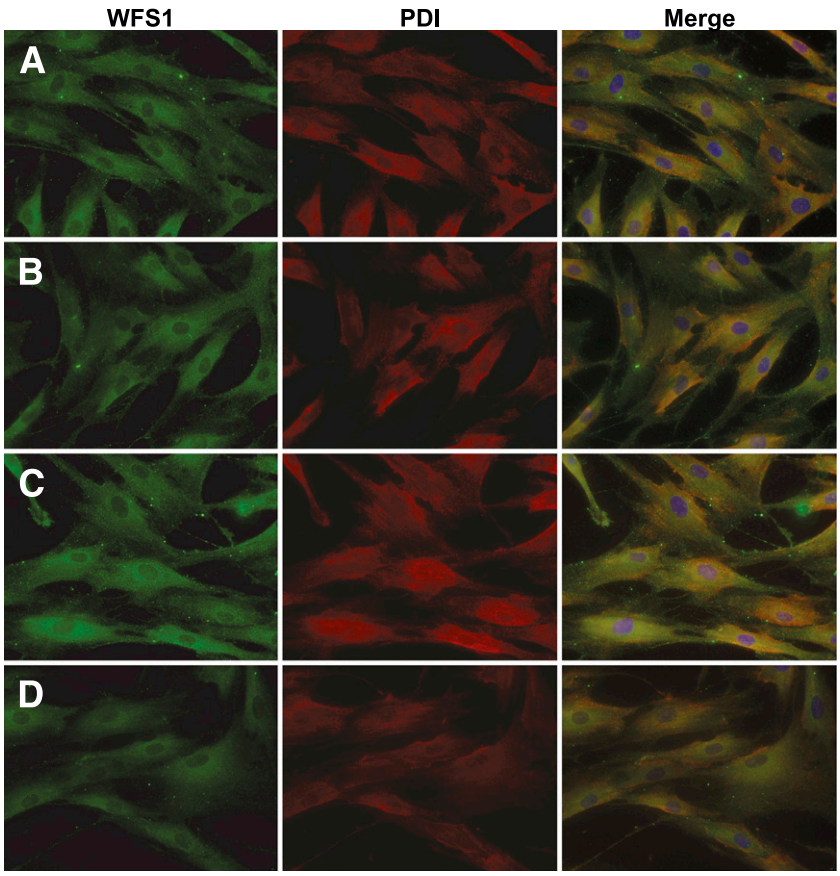


**FIG. 6. Cellular localization of WFS1. Skin fibroblasts obtained were double immunostained for WFS1 and PDI, and representative single-channel fluorescence images are shown individually and merged. III-1 (*A*), III-2: p.Trp314Arg (*B*), IV-1 (*C*), and IV-2: p.Trp314Arg (*D*). PDI, protein disulfide isomerase.**

insipidus, or deafness. The native WFS1 protein is a multimer of ~400 kDa and is likely a homo-oligomer of WFS1 monomers (30). Tetramers composed of purely wild-type monomers in this family would occur infrequently (1/16). Thus, it may be that tetramers composed of p.Trp314Arg mutant and wild-type monomers are not structurally competent or fully functional, leading to diabetes via a dominant-negative mechanism. Further investigation of this possibility may provide insight into the molecular effects of heterozygous mutations.

We believe this is the first complete report of dominant inheritance of an adult-onset diabetes phenotype (without other syndromic features of WS) associated with a missense mutation in *WFS1*. Recently, Johansson et al. (31) identified a single heterozygous *WFS1* missense mutation (encoding p.Arg703Cys) in a family with diabetes diagnosed early (14 years) and late (55 and 60 years) in life (Fig. 3*B*). However, whether p.Arg703Cys is the causative mutation in that family is unclear, as only three of the four affected family members tested were mutation carriers, and the ages of diabetes diagnoses were vastly different among the carriers.

The report cited above of de novo c.937C>T; p.His313Tyr mutations in two individuals with WS seems to indicate that WS can rarely be caused by heterozygous mutations. Interestingly, a single *WFS1* COOH-terminal missense variant (encoding p.Glu864Lys) has been identified to segregate dominantly in two unrelated families with Wolfram-like (WS-like) disorder (32,33), which is characterized by hearing impairment, diabetes, psychiatric illness, and variable optic atrophy (34). A small number of WS individuals have been identified to have a single heterozygous variant (EURO-WABB open variation database), but it is possible that a second unidentified variant may be present in these individuals.

Taken together, genetic variations in *WFS1* can lead to a spectrum of phenotypes, including susceptibility to type 1 diabetes, type 2 diabetes, WS, WS-like disorder, and SNHI. Genotype-phenotype correlations emerging from this work imply multiple roles of the WFS1 domains, where variant type and/or location can lead to differential clinical manifestations. In the case of p.Trp314Arg, heterozygous carriers have high penetrance development of adult-onset diabetes with relative insulin insufficiency, but the affected individuals lack other features of WS. Functionally, p.Trp314Arg appears to diminish the ability of WFS1 to protect against ER stress, which presumably damages β-cell function over time, leading to the onset of relative insulin insufficiency and diabetes.

## ACKNOWLEDGMENTS

This study was supported by the Intramural Research Program of the National Human Genome Research Institute, project 1ZIAHG000024 (F.S.C.); grants from the Academy of Finland (M.L.) and Finnish Diabetes Research Foundation (M.L.); National Institute of Diabetes and Digestive and Kidney Diseases grants DK-062370 (M.B.), DK-067493 (F.U.), DK-016746 (F.U.), 1K99-DK-092251 (M.L.S.), P30-DK-020579 (F.U.), and UL1-TR-000448 (F.U.); Juvenile Diabetes

Research Foundation Grant 47-2012-760 (F.U.); and American Diabetes Association Grant 1-12-CT-61 (F.U.).

No potential conflicts of interest relevant to this article were reported.

L.L.B. performed exome sequencing, variant validation, and screening; contributed to functional analyses; analyzed the sequence data; and contributed to the writing of the manuscript. P.S.C. developed and ran the analysis pipeline for NextGen sequence data and Illumina Omni2.5 data, contributed to the writing of the manuscript, and reviewed and edited the manuscript. T.H. and S.L. contributed to functional analyses. J.R.H. performed linkage analyses, contributed to the writing of the manuscript, and reviewed and edited the manuscript. A.J.S. performed exome sequencing, variant validation, and screening; contributed to functional analyses; and reviewed and edited the manuscript. P.H. and H.H. were responsible for the collection of clinical and laboratory data for the family and reviewed and edited the manuscript. J.M. and M.L.S. contributed to functional analyses and reviewed and edited the manuscript. S.P. was responsible for the collection of clinical and laboratory data for the family, generated fibroblast cultures from skin biopsies, and reviewed and edited the manuscript. P.N. was responsible for the collection of clinical and laboratory data for the family, designed and performed laboratory measures, and reviewed and edited the manuscript. N.N. and R.L.G. developed and ran the analysis pipeline for NextGen sequence data and Illumina Omni2.5 data and reviewed and edited the manuscript. M.B. supervised the genetic and linkage studies and their interpretation and reviewed and edited the manuscript. F.U. supervised the functional studies and their interpretation and reviewed and edited the manuscript. F.S.C. supervised the genetic and linkage studies and their interpretation, supervised the functional studies and their interpretation, and reviewed and edited the manuscript. M.L. was responsible for the collection of clinical and laboratory data for the family, supervised the genetic and linkage studies and their interpretation, and reviewed and edited the manuscript. F.S.C. is the guarantor of this work and, as such, had full access to all the data in the study and takes responsibility for the integrity of the data and the accuracy of the data analysis.

The authors are grateful to the Finnish individuals participating in this study. The authors would like to thank the following exome sequencing projects that produced and provided variant calls for comparison: *1*) the NHLBI GO Exome Sequencing Project and its ongoing studies, including the Lung GO Sequencing Project (HL-102923), the WHI Sequencing Project (HL-102924), the Broad GO Sequencing Project (HL-102925), the Seattle GO Sequencing Project (HL-102926), and the Heart GO Sequencing Project (HL-103010), and *2*) the T2D-GENES consortium (DK-085584, DK-085501, DK-085526, DK-085524, and DK-085545). The authors would also like to thank the National Intramural Sequencing Center Comparative Sequencing Program for sequence generation, Darryl Leja (National Institutes of Health, National Human Genome Research Institute, Bethesda, MD) for assistance with figure preparation, and Michael Erdos (National Institutes of Health, National Human Genome Research Institute, Bethesda, MD) for technical assistance and helpful discussions.

## REFERENCES

1. Molven A, Njølstad PR. Role of molecular genetics in transforming diagnosis of diabetes mellitus. Expert Rev Mol Diagn 2011;11:313–320
2. Steck AK, Winter WE. Review on monogenic diabetes. Curr Opin Endocrinol Diabetes Obes 2011;18:252–258
3. Ashcroft FM, Rorsman P. Diabetes mellitus and the β cell: the last ten years. Cell 2012;148:1160–1171
4. Vaxillaire M, Bonnefond A, Froguel P. The lessons of early-onset monogenic diabetes for the understanding of diabetes pathogenesis. Best Pract Res Clin Endocrinol Metab 2012;26:171–187
5. Teer JK, Bonnycastle LL, Chines PS, et al.; NISC Comparative Sequencing Program. Systematic comparison of three genomic enrichment methods for massively parallel DNA sequencing. Genome Res 2010;20:1420–1431
6. Wang K, Li M, Hakonarson H. ANNOVAR: functional annotation of genetic variants from high-throughput sequencing data. Nucleic Acids Res 2010;38:e164
7. Harrow J, Frankish A, Gonzalez JM, et al. GENCODE: the reference human genome annotation for The ENCODE Project. Genome Res 2012;22:1760–1774
8. 1000 Genomes Project Consortium, Abecasis GR, Auton A, Brooks LD, Depristo MA, Durbin RM, et al. An integrated map of genetic variation from 1,092 human genomes. Nature. 2012;491:56–65
9. Li H, Durbin R. Fast and accurate short read alignment with Burrows-Wheeler transform. Bioinformatics 2009;25:1754–1760
10. Ernst J, Kheradpour P, Mikkelsen TS, et al. Mapping and analysis of chromatin state dynamics in nine human cell types. Nature 2011;473:43–49
11. Purcell S, Neale B, Todd-Brown K, et al. PLINK: a tool set for whole-genome association and population-based linkage analyses. Am J Hum Genet 2007;81:559–575
12. Wigginton JE, Abecasis GR. PEDSTATS: descriptive statistics, graphics and quality assessment for gene mapping data. Bioinformatics 2005;21:3445–3447
13. Abecasis GR, Cherny SS, Cookson WO, Cardon LR. Merlin—rapid analysis of dense genetic maps using sparse gene flow trees. Nat Genet 2002;30:97–101
14. Fonseca SG, Ishigaki S, Oslowski CM, et al. Wolfram syndrome 1 gene negatively regulates ER stress signaling in rodent and human cells. J Clin Invest 2010;120:744–755
15. Fonseca SG, Fukuma M, Lipson KL, et al. WFS1 is a novel component of the unfolded protein response and maintains homeostasis of the endoplasmic reticulum in pancreatic beta-cells. J Biol Chem 2005;280:39609–39615
16. Fonseca SG, Urano F, Burcin M, Gromada J. Stress hypERactivation in the β-cell. Islets 2010;2:1–9
17. Rigoli L, Lombardo F, Di Bella C. Wolfram syndrome and WFS1 gene. Clin Genet 2011;79:103–117
18. Hansen L, Eiberg H, Barrett T, et al. Mutation analysis of the WFS1 gene in seven Danish Wolfram syndrome families; four new mutations identified. Eur J Hum Genet 2005;13:1275–1284
19. Fonseca SG, Urano F, Weir GC, Gromada J, Burcin M. Wolfram syndrome 1 and adenylyl cyclase 8 interact at the plasma membrane to regulate insulin production and secretion. Nat Cell Biol 2012;14:1105–1112
20. Awata T, Inoue K, Kurihara S, et al. Missense variations of the gene responsible for Wolfram syndrome (WFS1/wolframin) in Japanese: possible contribution of the Arg456His mutation to type 1 diabetes as a non-autoimmune genetic basis. Biochem Biophys Res Commun 2000;268:612–616
21. Zalloua PA, Azar ST, Delépine M, et al. WFS1 mutations are frequent monogenic causes of juvenile-onset diabetes mellitus in Lebanon. Hum Mol Genet 2008;17:4012–4021
22. Sandhu MS, Weedon MN, Fawcett KA, et al. Common variants in WFS1 confer risk of type 2 diabetes. Nat Genet 2007;39:951–953
23. Franks PW, Rolandsson O, Debenham SL, et al. Replication of the association between variants in WFS1 and risk of type 2 diabetes in European populations. Diabetologia 2008;51:458–463
24. Barrett TG, Bundey SE, Macleod AF. Neurodegeneration and diabetes: UK nationwide study of Wolfram (DIDMOAD) syndrome. Lancet 1995;346:1458–1463
25. Rigoli L, Di Bella C. Wolfram syndrome 1 and Wolfram syndrome 2. Curr Opin Pediatr 2012;24:512–517
26. Young TL, Ives E, Lynch E, et al. Non-syndromic progressive hearing loss DFNA38 is caused by heterozygous missense mutation in the Wolfram syndrome gene WFS1. Hum Mol Genet 2001;10:2509–2514
27. Bespalova IN, Van Camp G, Bom SJ, et al. Mutations in the Wolfram syndrome 1 gene (WFS1) are a common cause of low frequency sensorineural hearing loss. Hum Mol Genet 2001;10:2501–2508
28. Gürtler N, Kim Y, Mhatre A, et al. Two families with nonsyndromic low-frequency hearing loss harbor novel mutations in Wolfram syndrome gene 1. J Mol Med (Berl) 2005;83:553–560

29. Fukuoka H, Kanda Y, Ohta S, Usami S-I. Mutations in the WFS1 gene are a frequent cause of autosomal dominant nonsyndromic low-frequency hearing loss in Japanese. J Hum Genet 2007;52:510–515
30. Hofmann S, Philbrook C, Gerbitz K-D, Bauer MF. Wolfram syndrome: structural and functional analyses of mutant and wild-type wolframin, the WFS1 gene product. Hum Mol Genet 2003;12:2003–2012
31. Johansson S, Irgens H, Chudasama KK, et al. Exome sequencing and genetic testing for MODY. PLoS ONE 2012;7:e38050
32. Eiberg H, Hansen L, Kjer B, et al. Autosomal dominant optic atrophy associated with hearing impairment and impaired glucose regulation caused by a missense mutation in the WFS1 gene. J Med Genet 2006;43:435–440
33. Valéro R, Bannwarth S, Roman S, Paquis-Flucklinger V, Vialettes B. Autosomal dominant transmission of diabetes and congenital hearing impairment secondary to a missense mutation in the WFS1 gene. Diabet Med 2008;25:657–661
34. Tranebjaerg L, Barrett T, Rendtorff ND. *WFS1*-related disorders. In *GeneReviews*. GeneReviews. Pagon RA, Ed. Seattle, WA, University of Washington, Seattle, p. 1–19